Heterogeneous Catalysis

DOI: 10.1002/ange.201210077

Importance of the Metal–Oxide Interface in Catalysis: In Situ Studies of the Water–Gas Shift Reaction by Ambient-Pressure X-ray Photoelectron Spectroscopy**

*Kumudu Mudiyanselage, Sanjaya D. Senanayake, Leticia Feria, Shankhamala Kundu, Ashleigh E. Baber, Jesús Graciani, Alba B. Vidal, Stefano Agnoli, Jaime Evans, Rui Chang, Stephanus Axnanda, Zhi Liu, Javier F. Sanz, Ping Liu, José A. Rodriguez, and Darío J. Stacchiola**

The traditional approach to the optimization of metal/oxide catalysts has focused on the properties of the metal and the selection of the proper oxide for its dispersion. The importance of metal–oxide interfaces has long been recognized,[1] but the molecular determination of their properties and role is only now emerging.[2] Atoms with properties ranging from metallic to ionic are available at the interface and create unique reaction sites. We show herein how sites associated with a metal–ceria interface can dramatically change the reaction mechanism of the water–gas shift reaction (WGSR; $CO + H_2O \rightarrow H_2 + CO_2$). The WGSR is critical in the production of hydrogen. Multiple reaction mechanisms have been proposed.[3] In the redox mechanism, CO reacts with oxygen derived from the dissociation of H_2O. In the associative process, the formation of a carbonaceous CO_xH_y intermediate must precede the production of H_2 and CO_2. In situ studies are essential for the detection of surface species and active phases only present under the reaction conditions.[4] We present a combination of near-ambient-pressure X-ray photoelectron spectroscopy (NAP XPS), infrared reflection absorption spectroscopy (IRRAS), and density functional theory (DFT) calculations used to study the WGSR on CeO_x nanoparticles deposited on Cu(111) and Au(111). Under WGSR conditions, adsorbed bent carboxylate ($CO_2^{\delta-}$) species were identified over both CeO_x/Cu(111) and CeO_x/Au(111), with the ceria in a highly reduced state. By combining in situ experimental results with calculations, we show that the precursor for the formation of $CO_2^{\delta-}$ is a carboxy (HOCO) intermediate on the metal–oxide interface.

The WGSR has been investigated at the molecular level over single crystals.[5] To establish the importance of the morphology and electronic structure of oxide nanoparticle–metal interfaces, inverse (oxide/metal) model catalysts have been introduced.[6] Au(111) is inactive for the WGSR but can be activated in the presence of CeO_x nanoparticles.[6a] A large enhancement in activity was also found on CeO_x/Cu(111);[6b] Cu(111) is a typical benchmark for WGSR studies.[6] The rate of H_2 production over these catalysts is compared in Figure 1. Why are the CeO_x/Cu(111) and CeO_x/Au(111) catalysts highly active?

The dissociation of H_2O is considered to be the rate-determining step in the WGSR.[3c] Water does not dissociate

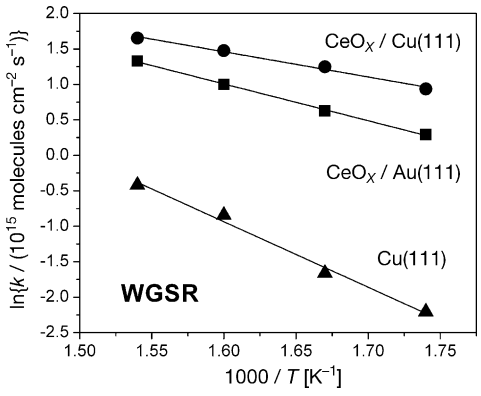

Figure 1. Arrhenius plots of the WGSR rate (CO: 20 Torr, H_2O: 10 Torr) on clean Cu(111), CeO_x/Cu(111), and CeO_x/Au(111).

[*] Dr. K. Mudiyanselage, Dr. S. D. Senanayake, Dr. S. Kundu, Dr. A. E. Baber, Dr. J. Graciani, Dr. A. B. Vidal, Dr. S. Agnoli, Dr. P. Liu, Dr. J. A. Rodriguez, Dr. D. J. Stacchiola
Chemistry Department, Brookhaven National Laboratory
Upton, NY 11973 (USA)
E-mail: djs@bnl.gov
Dr. L. Feria, Dr. J. Graciani, Prof. J. F. Sanz
Departamento de Química Física, Universidad de Sevilla
41012 Seville (Spain)
Prof. J. Evans
Facultad de Ciencias, Universidad Central de Venezuela
Caracas 1020A (Venezuela)
Dr. R. Chang
Shanghai Institute of Microsystem and Information Technology
Shanghai 200050 (China)
Dr. S. Axnanda, Dr. Z. Liu
The Advanced Light Source, Lawrence Berkeley National Laboratory
Berkeley, CA 94720 (USA)

[**] Research carried at BNL was financed by the US DOE, Office of BES (Grant No. DE-AC02-98CH10086). Some of the calculations were performed at the Center for Functional Nanomaterials at BNL. The main theoretical part was carried out by the group of J.F.S. and funded by the Ministerio de Economía y Competitividad (Spain, grants MAT2012-31526 and CSD2008-0023). Computational resources were provided by the Barcelona Centro Nacional de Supercomputación (Spain). J.E. thanks INTEVEP and IDB for grants used for the research in Venezuela.

Supporting information for this article is available on the WWW under http://dx.doi.org/10.1002/anie.201210077.

on Cu(111) even under NAP conditions,[7] and theory predicts a large barrier for the process.[3c,8] When H_2O is adsorbed over reduced-CeO_x/Cu(111), the formation of hydroxy (OH) groups bound to CeO_x is observed.[7a] O vacancies promote the dissociation.[9] Figure 2 shows the IRRA spectra for

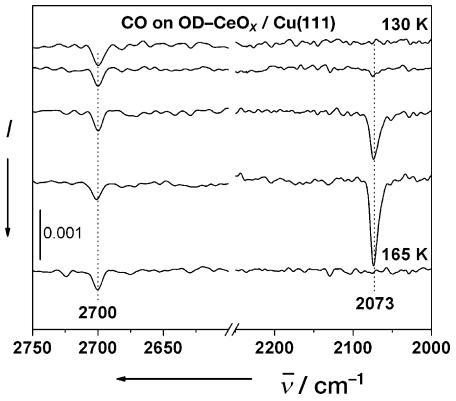

Figure 2. Adsorption of CO on OD-covered reduced-CeO_x/Cu(111) at 130 K as a function of CO exposure. Bottom spectrum: Annealing at 165 K.

coadsorbed CO and OD on reduced-CeO_x/Cu(111) under ultrahigh vacuum (UHV). The peak at 2073 cm^{-1} was assigned to CO in atop sites on Cu(111), and the peak at 2700 cm^{-1} to OD isolated on CeO_x.[10] In contrast, CO and OD interact when coadsorbed on Cu(111) or Au(111).[11] Annealing of the CO- and OD-covered surface at 165 K induces the desorption of CO and thus prevents its reaction with OD under UHV. Theory predicts the formation of an HOCO intermediate.[3a,c] This process may take place if chemisorbed CO is present in a dynamic equilibrium. Surface-bound formate (HCOO)[12] or carbonate (CO_3)[3b,12] species could also be formed as intermediates.

NAP XPS experiments were performed under WGSR conditions. Figure 3 shows spectra obtained during the WGSR (CO: 90 mTorr, H_2O: 30 mTorr) with features due to gas-phase CO and H_2O.[13] On Cu(111), a broad peak at 533.4 eV in the O 1s spectrum and the main peak in the C 1s spectrum at 286.2 eV were assigned to chemisorbed CO.[14] Features at 285 eV and below in the C 1s spectra are associated with C_xH_y species (referred as C_0) formed from residual gases, as described in previous reports.[13] No other features are observed at higher temperatures in the presence of CO and H_2O. Therefore, our data do not support an associative mechanism for the WGSR on Cu(111), since no surface species other than CO are observed under the reaction conditions or in the presence of CO and H_2O at elevated pressures. This result is in agreement with those of previous ex situ studies.[5a]

When CeO_x nanoparticles are deposited on Cu(111), changes in the O and C 1s regions are observed under WGSR conditions. The O 1s peak at 530.0 eV in Figure 3b is from the CeO_x nanoparticles.[7a] The broad peak at 531.8 eV is associated with OH groups, and a shoulder at a higher binding energy (BE) corresponds to adsorbed CO. Our UHV studies

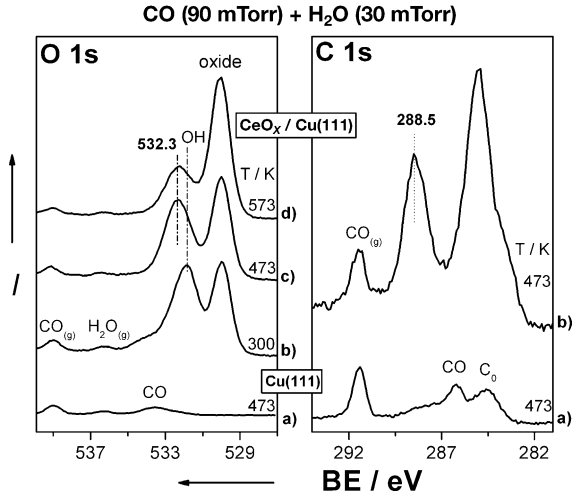

Figure 3. NAP XPS of Cu(111) and CeO_x/Cu(111) under WGSR conditions.

have shown that OH groups on Cu(111) are observed at 531.5 and at 532.4 eV on CeO_x/Cu(111).[7a] In the presence of oxygen on Cu(111), as in the as-prepared CeO_x/Cu(111) sample, OH groups can be formed and stabilized at 300 K when exposed to H_2O.[7b] Thus, the peak observed at 531.8 eV is due to OH groups on both the ceria nanoparticles and Cu(111). As the sample temperature was increased, several changes were observed. In the O 1s spectrum (Figure 3c), the shoulder due to chemisorbed CO and the peak at 531.8 eV, mainly due to OH on Cu(111), decreased in intensity, and a peak at 532.3 eV became dominant. The peak at 532.3 eV could be assigned to numerous adsorbed species, including CO_3, HCOO, $CO_2^{\delta-}$, and OH on CeO_x. The reduction of Cu_2O/Cu(111) by exposure to CO at elevated temperatures is facile,[15] and under WGSR conditions all the Cu is present as Cu^0. Ce 4d spectra revealed reduction of the CeO_x nanoparticles during the reaction (see Figure S1 in the Supporting Information). The C 1s spectrum (Figure 3b) showed a peak at 288.5 eV and a C_0 peak at approximately 285 eV.

The assignment of the peak at 288.5 eV is challenging. Formate is ruled out, since its C 1s BEs on CeO_x/Cu(111) are 289.2 and 287.5 eV on CeO_x and Cu(111), respectively (formate species were prepared by the exposure of CeO_x/Cu(111) to formic acid, HCOOH; see Figure S2 in the Supporting Information). Adsorbed formate on CeO_2 films has a BE of 289 eV.[16] We can also rule out CO_3 species, which have a C 1s BE of about 289.5 eV.[6c,11,16] We therefore tentatively assigned the peak at 288.5 eV to a $CO_2^{\delta-}$ or HOCO species. A $CO_2^{\delta-}$ species was reported to result from the adsorption of CO_2 on metals under an UHV at low temperatures[17] and on Cu foil at 300 K and NAP, with a BE of 288.4 eV.[13b] As IRRA spectra of this $CO_2^{\delta-}$ species have been well characterized,[18] we could unequivocally show its presence on the reduced-CeO_x/Cu(111) system upon exposure to CO_2 (see Figure S3), together with a small signal due to a CO_3 species. Since the C 1s XPS spectra indicate that the C atom of the carboxylate sits on a Cu atom, the ν_{asym}(OCO) mode observed in the IRRAS shows that the $CO_2^{\delta-}$ species has broken C_{2v} symmetry; that is, the two oxygen atoms are

not equivalent. The corresponding C 1 s spectrum presents a mixture of $CO_2^{\delta-}$ and CO_3 species, in analogy with the results obtained on Cu foil (see Figure S4 and Ref. [13b]). On the basis of the above results, the peak at 288.5 eV in Figure 3 b was assigned to a $CO_2^{\delta-}$ species.

$CO_2^{\delta-}$ adsorbed on Cu has an O 1s BE of 531.4 eV.[13b] Carbonaceous species adsorbed on ceria have higher BEs than those on metal surfaces. For example, the O 1 s peak of formate species shifts from 531.4 eV on Cu (the same value as that found for $CO_2^{\delta-}$)[13b] to 533.2 eV on CeO_x nanoparticles[6c] (see Table S1 in the Supporting Information). Therefore, the observed peak at 532.3 eV in Figure 3 c suggests that the $CO_2^{\delta-}$ species is adsorbed at the interface between Cu(111) and the CeO_x nanoparticles, in agreement with the IRRAS data. Annealing of the sample at the optimal WGSR temperature (573 K; Figure 3 d) induced a decrease in the number of surface species. Upon evacuation (while maintaining the temperature of the sample at 573 K), all peaks, except that for C_0, disappeared, which indicates that the $CO_2^{\delta-}$ species is stabilized only under WGSR conditions.

In contrast to the observations on Cu(111), where no surface species other than CO were detected during the WGSR, on CeO_x/Cu(111) the presence of stable CO_xH_y species was clearly established, and these species were identified as $CO_2^{\delta-}$. We conclude that on the CeO_x/Cu(111) system, the WGSR occurs by an associative mechanism, which leads to the formation of $CO_2^{\delta-}$. Since this species is not observed on either CeO_2 films (see Figure S5) or clean Cu(111), the interfacial sites formed on the CeO_x/Cu(111) system appear to be critical for the formation and stabilization of $CO_2^{\delta-}$.

The reaction of CO and H_2O over reduced-CeO_x/Au(111) under UHV conditions has also been studied previously. H_2O dissociates on the reduced-CeO_x/Au(111) system to form OH groups, which are stable up to 560 K.[7a] The interaction of CO with preadsorbed OH species leads to the production of surface HCOO and CO_3 in the presence of Ce^{3+} at high concentrations in the ceria nanoparticles. In contrast, HCOO or CO_3 species were not observed to result from the CO + OH interaction over reduced-CeO_x/Cu(111) under UHV conditions. This result demonstrates that the metal–oxide interface and the electronic properties of the oxide nanoparticles differ among metals and affect this critical associative reaction step (CO + OH).

NAP XPS experiments under CO (300 mTorr) and H_2O (100 mTorr) showed no surface species on Au(111) in the temperature range 300–573 K (Figure 4). CeO_x nanoparticles deposited on the Au(111) surface were exposed to CO (10–300 mTorr) during annealing from 300 to 573 K. Figure 4 b (C 1s) shows a peak at 289.3 eV, which was assigned to CO_3 species formed on CeO_x.[6c,13b] Exposure to CO at 300 mTorr did not lead to new surface species. Figure 4 c shows the result of exposing the CeO_x/Au(111) surface to CO (12 mTorr) and H_2O (4 mTorr) at 300 K. Without the hindrance of $CO_{(g)}$ or $H_2O_{(g)}$, the formation of surface species is visible. The main feature in the C 1s region at 288.3 eV, with a shoulder at higher BEs, is similar to the case on CeO_x/Cu(111) system discussed above and it is assigned to $CO_2^{\delta-}$ species. At higher pressures and temperatures (Figure 4 d), $CO_{(g)}$, $H_2O_{(g)}$, and

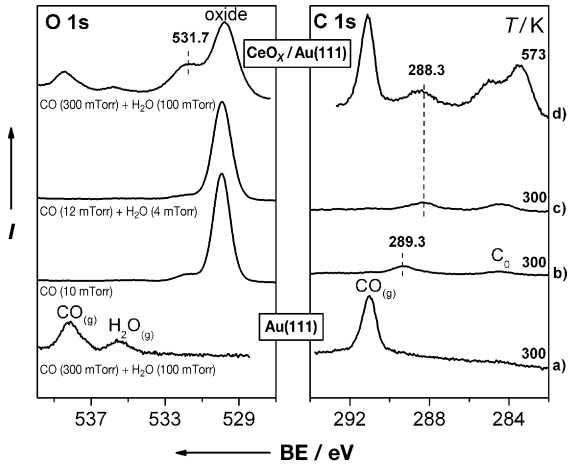

Figure 4. NAP XPS of Au(111) and CeO_x/Au(111) under WGSR conditions.

changes in the main features were observed. A shift to higher BEs of the feature at 288.3 eV in the C 1s region can be explained by the presence of $CO_2^{\delta-}$ and the formation of HCOO on the ceria nanoparticles; HCOO appears at approximately 289 eV in the spectrum.[7a] In the O 1s region, a large feature centered at 531.7 eV is due to a combination of OH, HCOO, and $CO_2^{\delta-}$ species. Higher pressures of reactants and higher temperatures led in the case of CeO_x/Au(111) to the formation of formate species, but not for CeO_x/Cu(111), which presents a stronger oxide–metal interaction. This behavior is directly comparable to that of powder catalysts based on Cu and CeO_2, for which no evidence of formate species was observed during the WGSR by IR spectroscopy.[19] However, from powder samples it cannot be determined whether $CO_2^{\delta-}$ is present on the catalyst owing to the strong peaks of carbonate species always present on these samples, which mask the presence of $CO_2^{\delta-}$.[19] During the WGSR, reduction of the CeO_x nanoparticles from $CeO_{1.98}$ to $CeO_{1.79}$ was observed (see Figure S6). The effect of a mixture of CO (12 mTorr) and H_2O (4 mTorr) on a film of 5 monolayers of CeO_x was also investigated: a strong formate feature was observed at 288.9 eV and remained up to a temperature of 600 K (see Figure S5).

Figure 5 shows the calculated energy profile for the WGSR on a CeO_x/Cu(111) surface. The adsorption energy of water is exothermic (−0.53 eV). The dissociation of water is very facile, as the activation barrier is only 0.22 eV, and the process is exothermic by −0.34 eV. The same process on the Cu(111) surface leads to a very high activation barrier of 1.0–1.4 eV.[3c,8] On CeO_x/Cu(111), the activation barrier for the dissociation of water is lowered dramatically, to the point that the dissociation of water may no longer be the rate-limiting step as traditionally accepted.

The adsorption of CO in the vicinity of the oxide particles is exothermic (−0.47 eV). On the reaction pathway via the carboxy species, the formation of HOCO is endothermic (0.39 eV), and the required activation barrier for the process at the interface is 0.41 eV. The analogous process on clean Cu(111) is in this case very similar (0.61 eV on Cu(111)),

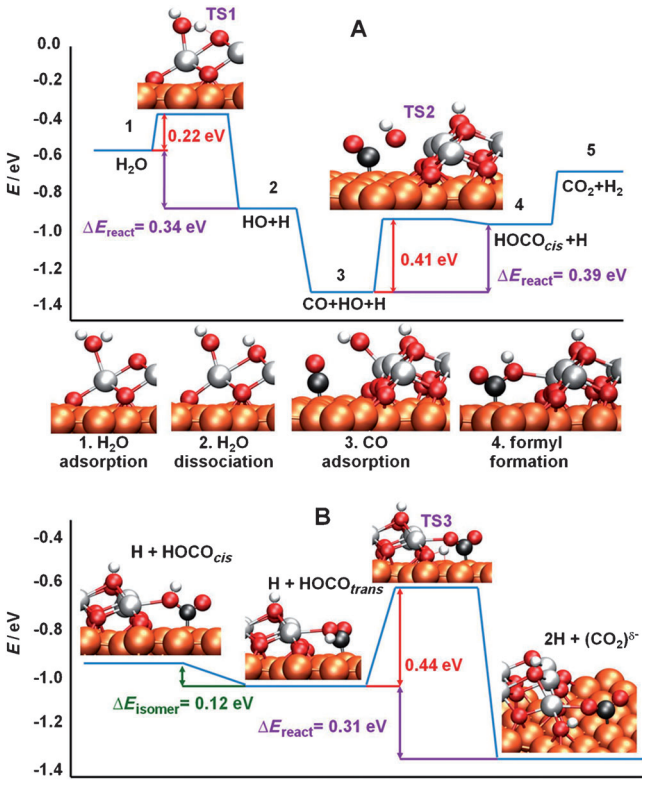

Figure 5. Structures and energies for the WGSR on CeO_x/Cu(111). A) Proposed pathway. E_{react} stands for reaction energy and TS for transition state. Energy barriers are in red. B) Pathway for the formation of $CO_2^{\delta-}$ at the CeO_x/Cu interface from adsorbed HOCO species.

although the barrier on CeO_x/Cu(111) remains lower. From this intermediate, the reaction to form H_2 and CO_2 is endothermic by only 0.3 eV. The whole reaction path is shown in Figure 5A. Fundamental steps that occur at the metal–oxide interface are shown in Figure 5B.

CO_2 generated by the deprotonation of HOCO can be trapped on the surface of the catalyst, as shown in Figure 5B. HOCO initially has a *cis* conformation with the H atom pointing upward. To be deprotonated, the OH group has to rotate to a *trans* configuration. Both adsorbed isomers have a similar energy. From this configuration, HOCO can transfer the H atom to an oxygen atom on the oxide particle exothermically (−0.31 eV) with a low activation barrier of 0.44 eV. The final products are two H atoms adsorbed on the oxide particle and one CO_2 species adsorbed on the metal surface, whereby one of its oxygen atoms interacts with the oxide particle. CO_2 desorbs readily from the metal surface and can only remain on the surface if it receives charge transfer from the oxide to become a $CO_2^{\delta-}$ species. This behavior can be seen indirectly from the adsorption geometry. CO_2 is linear in the gas phase, but here it adopts a bent geometry. In contrast to the behavior of CO_2 on Cu(111) surfaces, this $CO_2^{\delta-}$ species was found to be very stable, as the desorption to form CO_2 and H_2 in the gas phase is an endothermic process that requires 0.73 eV. The calculated vibrational-frequency shift in the ν_{asym}(OCO) mode from gas-phase CO_2 to the interfacial $CO_2^{\delta-}$ matches the experimentally observed shift of approximately 700 cm^{-1} (see Figure S3 and Table S2). We also carried out calculations on CeO_x/Au(111) and found that the CO_2 can be stabilized at the interface between a Ce^{3+} and a Au atom, with a bent configuration and partial electron transfer to the $CO_2^{\delta-}$ species of 0.55 electrons. The desorption of H_2 and CO_2 has to be a concerted reaction in which the electron trapped at the $CO_2^{\delta-}$ species is released and transferred to the adsorbed H atoms to form H_2. The release of the charge enables the desorption of CO_2 and at the same time enables the formation of H_2 (which needs to recover two electrons from the system before it can form and desorb). The pathway for the formation of products in the WGSR does not necessarily have to pass through the formation of $CO_2^{\delta-}$, since HOCO species can evolve to CO_2 and H_2 directly, but we have shown that the formation of the $CO_2^{\delta-}$ species from a carboxy intermediate is indeed possible, and the high stability of the $CO_2^{\delta-}$ species can help to rationalize the experimental findings.

The most abundant surface species on Cu(111) under WGSR conditions is adsorbed CO, which suggests that the prevailing reaction path is not an associative mechanism. Under mild WGSR conditions, trapped $CO_2^{\delta-}$ species were identified over both CeO_x/Cu(111) and CeO_x/Au(111) systems, and the reduction of Ce^{4+} to Ce^{3+} (Ce 4d) was observed. NAP XPS and DFT calculations showed that $CO_2^{\delta-}$ derived from a carboxy intermediate is stabilized at the interfaces of CeO_x/Cu(111) and CeO_x/Au(111). Even though the WGSR over CeO_x/Cu catalysts can occur by both redox and associative mechanisms, the study presented herein shows that the presence of the oxide–metal interface activates the more efficient associative mechanism pathway and leads to an increase by more than one order of magnitude in the activity of the CeO_x/Cu(111) system relative to that of Cu(111). The observed results also indicate that formate species are not likely to be key intermediates in the WGSR over CeO_x/Cu(111), CeO_x/Au(111), or Cu–CeO_x powder catalysts.

Our study illustrates the power of in situ mechanistic studies on well-defined catalysts and the important role that metal–oxide interfaces can play in catalysis. The simultaneous participation of atoms present on the metal and the oxide make possible the formation of HOCO and $CO_2^{\delta-}$ and thus favors a reaction mechanism for hydrogen production that is not effective on isolated copper or isolated ceria. Thus, when optimizing this type of catalyst, one must pay special attention to the properties of the metal–oxide interface.

Experimental Section

NAP XPS studies were performed at the Advanced Light Source in Berkeley, CA (beamline 9.3.2). A VG Scienta R4000 HiPP analyzer was used.[20] Traps were utilized along gas lines. The O 1s region was probed with a photon energy of 700 eV, and the C 1s, Cu 3s, and Ce 4d regions with a photon energy of 490 eV and a resolution of 0.2–0.3 eV. Calibrations were performed with the Cu 3s or the Au 4f7/4 peaks. IRRAS was performed in a combined UHV/elevated-pressure cell system with a Bruker IFS 66v/S spectrometer.[21] Spectra were collected at a resolution of 4 cm^{-1} by using a grazing angle. Crystals were cleaned with cycles of Ar^+ sputtering (1 kV, 300 K), heating to 900 K, and annealing. Ceria was deposited by the evaporation of Ce

metal in O_2 (5×10^{-7} Torr) at 550 K, and reduced-CeO_x was deposited by using O_2 (2×10^{-8} Torr) at 550 K. The coverage of CeO_x was 0.1–0.2 monolayers. All calculations were performed within the framework of DFT, as implemented in the Vienna Ab Initio Simulation Program (VASP 4.6). Details are presented in the Supporting Information.

Received: December 18, 2012
Revised: March 1, 2013
Published online: April 9, 2013

Keywords: ceria · heterogeneous catalysis · nanocatalysis · surface chemistry · water–gas shift reaction

[1] a) G. M. Schwab, *Angew. Chem.* **1967**, *79*, 325 – 326; *Angew. Chem. Int. Ed. Engl.* **1967**, *6*, 375; b) K. Hayek, R. Kramer, Z. Paal, *Appl. Catal. A* **1997**, *162*, 1 – 15.

[2] a) J. Libuda, H. J. Freund, *Surf. Sci. Rep.* **2005**, *57*, 157 – 298; b) I. X. Green, W. J. Tang, M. Neurock, J. T. Yates, *Science* **2011**, *333*, 736 – 739.

[3] a) P. Liu, J. A. Rodriguez, *J. Chem. Phys.* **2007**, *126*, 164705; b) A. B. Mhadeshwar, D. G. Vlachos, *J. Phys. Chem. B* **2004**, *108*, 15246; c) A. A. Gokhale, J. A. Dumesic, M. Mavrikakis, *J. Am. Chem. Soc.* **2008**, *130*, 1402 – 1414; d) R. Burch, A. Goguet, F. C. Meunier, *Appl. Catal. A* **2011**, *409*, 3 – 12.

[4] M. Salmeron, R. Schlögl, *Surf. Sci. Rep.* **2008**, *63*, 169 – 199.

[5] a) J. Nakamura, J. M. Campbell, C. T. Campbell, *J. Chem. Soc. Faraday Trans.* **1990**, *86*, 2725 – 2734; b) J. A. Rodriguez, P. Liu, J. Hrbek, J. Evans, M. Pérez, *Angew. Chem.* **2007**, *119*, 1351 – 1354; *Angew. Chem. Int. Ed.* **2007**, *46*, 1329 – 1332; c) J. B. Park, J. Graciani, J. Evans, D. Stacchiola, S. G. Ma, P. Liu, A. Nambu, J. F. Sanz, J. Hrbek, J. A. Rodriguez, *Proc. Natl. Acad. Sci. USA* **2009**, *106*, 4975 – 4980.

[6] a) J. A. Rodriguez, S. Ma, P. Liu, J. Hrbek, J. Evans, M. Pérez, *Science* **2007**, *318*, 1757 – 1760; b) J. A. Rodriguez, J. Graciani, J. Evans, J. B. Park, F. Yang, D. Stacchiola, S. D. Senanayake, S. G. Ma, M. Pérez, P. Liu, J. F. Sanz, J. Hrbek, *Angew. Chem.* **2009**, *121*, 8191 – 8194; *Angew. Chem. Int. Ed.* **2009**, *48*, 8047 – 8050; c) S. D. Senanayake, D. Stacchiola, J. Evans, M. Estrella, L. Barrio, M. Pérez, J. Hrbek, J. A. Rodriguez, *J. Catal.* **2010**, *271*, 392 – 400.

[7] a) S. D. Senanayake, J. T. Sadowski, J. Evans, S. Kundu, S. Agnoli, F. Yang, D. Stacchiola, J. I. Flege, J. Hrbek, J. A. Rodriguez, *J. Phys. Chem. Lett.* **2012**, *3*, 839 – 843; b) S. Yamamoto, K. Andersson, H. Bluhm, G. Ketteler, D. E. Starr, T. Schiros, H. Ogasawara, L. G. M. Pettersson, M. Salmeron, A. Nilsson, *J. Phys. Chem. C* **2007**, *111*, 7848 – 7850.

[8] J. L. C. Fajín, F. Illas, J. R. B. Gomes, *J. Chem. Phys.* **2009**, *130*, 224702.

[9] V. Matolín, I. Matolínová, F. Dvořák, V. Johánek, J. Mysliveček, K. C. Prince, T. Skála, O. Stetsovych, N. Tsud, M. Václavů, B. Šmíd, *Catal. Today* **2012**, *181*, 124 – 132.

[10] P. Hollins, J. Pritchard, *Surf. Sci.* **1979**, *89*, 486 – 495.

[11] S. D. Senanayake, D. Stacchiola, P. Liu, C. B. Mullins, J. Hrbek, J. A. Rodriguez, *J. Phys. Chem. C* **2009**, *113*, 19536 – 19544.

[12] R. Burch, *Phys. Chem. Chem. Phys.* **2006**, *8*, 5483 – 5500.

[13] a) X. Y. Deng, J. Lee, C. J. Wang, C. Matranga, F. Aksoy, Z. Liu, *J. Phys. Chem. C* **2010**, *114*, 22619 – 22623; b) X. Y. Deng, A. Verdaguer, T. Herranz, C. Weis, H. Bluhm, M. Salmeron, *Langmuir* **2008**, *24*, 9474 – 9478.

[14] H. Tillborg, A. Nilsson, N. Mårtensson, *J. Electron Spectrosc. Relat. Phenom.* **1993**, *62*, 73 – 93.

[15] F. Yang, Y. Choi, P. Liu, D. Stacchiola, J. Hrbek, J. A. Rodriguez, *J. Am. Chem. Soc.* **2011**, *133*, 11474 – 11477.

[16] S. D. Senanayake, D. R. Mullins, *J. Phys. Chem. C* **2008**, *112*, 9744 – 9752.

[17] G. Illing, D. Heskett, E. W. Plummer, H. J. Freund, J. Somers, T. Lindner, A. M. Bradshaw, U. Buskotte, M. Neumann, U. Starke, K. Heinz, P. L. Deandres, D. Saldin, J. B. Pendry, *Surf. Sci.* **1988**, *206*, 1 – 19.

[18] a) O. Seiferth, K. Wolter, B. Dillmann, G. Klivenyi, H. J. Freund, D. Scarano, A. Zecchina, *Surf. Sci.* **1999**, *421*, 176 – 190; b) H. J. Freund, M. W. Roberts, *Surf. Sci. Rep.* **1996**, *25*, 225 – 273.

[19] X. Q. Wang, J. A. Rodriguez, J. C. Hanson, D. Gamarra, A. Martínez-Arias, M. Fernández-García, *J. Phys. Chem. B* **2006**, *110*, 428 – 434.

[20] M. E. Grass, P. G. Karlsson, F. Aksoy, M. Lundqvist, B. Wannberg, B. S. Mun, Z. Hussain, Z. Liu, *Rev. Sci. Instrum.* **2010**, *81*, 053106.

[21] J. Hrbek, F. M. Hoffmann, J. B. Park, P. Liu, D. Stacchiola, Y. S. Hoo, S. Ma, A. Nambu, J. A. Rodriguez, M. G. White, *J. Am. Chem. Soc.* **2008**, *130*, 17272 – 17273.

